OXFORD Toxicology Research

Toxicology Research, 2025, **14**, tfaf064
https://doi.org/10.1093/toxres/tfaf064
Paper

In vitro investigation of the toxicological mechanisms of Fingolimod (S)-phosphate in HEPG2 cells

Ayşenur Bilgehan[1,2], Zehra Şeker[2], Mohammed T. Qaoud[3] and Gül Özhan[1,*]

[1]Faculty of Pharmacy, Department of Pharmaceutical Toxicology, Istanbul University, Fatih, Istanbul 34116, Türkiye,
[2]Institute of Graduate Studies in Health Sciences, Istanbul University, Fatih, Istanbul 34116, Türkiye,
[3]Faculty of Pharmacy, Department of Pharmacy, Cyprus International University, Nicosia, Northern Cyprus 99258, Türkiye
*Corresponding author. Faculty of Pharmacy, Department of Pharmaceutical Toxicology, Istanbul University, Istanbul 34116, Türkiye, (Email: gulozhan@istanbul.edu.tr)

Fingolimod (FTY720) was the first sphingosine-1-phosphate (S1P) receptor modulator approved by the US Food and Drug Administration for the treatment of multiple sclerosis. The active form, FTY720 (S)-P, acts as a potent agonist of the S1P receptor, leading to its downregulation on the cell surface, reduced activity, and termination of sphingosine-dependent intracellular signalling. Elevated hepatic enzyme levels, clinically significant liver injury, and acute liver failure have been observed in patients treated with FTY720 (S)-P, which requires additional monitoring. This is the first study to investigate the mechanisms underlying the hepatotoxicity of FTY720 (S)-P and represents an important contribution to elucidating its toxicity mechanisms in the human hepatocellular carcinoma cell line HepG2. Following a 72-h exposure, standard methods were used to evaluate specific targets, including cytotoxic effect potentials, mitochondrial parameters, and changes of the antioxidant enzyme levels. FTY720 (S)-P exposure resulted in time- and dose-dependent decreases in cell viability, mitochondrial membrane potential, and ATP levels, as well as the induction of oxidative stress. The complex toxic profile observed for FTY720 (S)-P is hypothesized to originate from its interaction with sirtuin proteins, particularly SIRT3 and SIRT5. It was also complemented with molecular docking simulations to assess the compound's targeting potential by analysing its interaction profile and binding pose within the active sites of both proteins. The results supported the proposed hypothesis, demonstrating an optimal fitting profile and favourable interaction behaviour within the binding pockets of the SIRT3 and SIRT5 enzymes.

Keywords: Fingolimod; oxidative stress; hepatotoxicity.

Introduction

Multiple sclerosis (MS) is the leading cause of non-traumatic neurological dysfunction among young adults. Effective management of MS necessitates comprehensive strategy to control acute episodes, manage progressive deterioration, and alleviate troublesome or incapacitating symptoms. Significant advancements in the treatment of MS have improved the long-term outlook for many patients. Higher-efficacy drugs requiring less frequent administration have emerged as the preferred options due to better tolerability and adherence.

Interferons, glatiramer acetate, teriflunomide, sphingosine-1-phosphate (SIP) receptor modulators, fumarates, cladribine, and three varieties of monoclonal antibodies are among the pharmaceuticals. [1] Relapsing–remitting MS is the most commonly encountered form of MS. The condition is characterised by episodes of inflammation that target both the myelin and nerve fibres of the central nervous system. The episodes result in small areas of damage that cause the symptoms associated with MS.[2]

Fingolimod (FTY720) is a small molecule that is lipid-soluble and derived from a metabolite of the *Isaria sinclairii* fungus. It is structurally similar to the naturally occurring sphingosine and it works in a unique way by triggering a natural control pathway that prevents the movement of lymphocytes and causes them to be redistributed in a specific manner. Like sphingosine, FTY720 is converted into its active form, FTY720 phosphate (FTY720 (S)-P), through phosphorylation by the liver enzyme sphingosine kinase 2 (SphK2). This active metabolite is structurally similar to SIP and acts as a SIP receptor modulator, then binds to four subtypes of S1P receptor: S1P1, S1P3, S1P4, and S1P5. It acts as a functional agonist, initially activating lymphocyte S1P1 through high-affinity receptor binding and subsequently inducing S1P1 downregulation. As a result, lymphocytes become unable to receive the S1P signal that is required to leave the lymph nodes and enter inflamed tissue.[3,4] This reduces the infiltration of auto aggressive lymphocytes into the central nervous system and demonstrates immunosuppressive activity.[3,5,6] Thus, the mechanism of action of FTY720 relies on reducing the number of circulating lymphocytes, which prevents them from entering the central nervous system, and thereby preventing inflammation and damage.[3] In late 2010, FDA approved FTY720 as the first oral disease-modifying drug for the treatment of relapsing–remitting MS.[7,8]

FTY720 has been shown to reduce the relapse rate and delay disability progression in patients with relapsing–remitting MS, compared to placebo or other disease-modifying drugs. A randomized, double-blind, placebo-controlled trial was conducted to evaluate the efficacy and safety of FTY720 in patients with relapsing–remitting MS. The study demonstrated that FTY720 notably decreased the annualized relapse rate and lowered the risk of disability progression compared to placebo. The drug also reduced the number of gadolinium-enhancing lesions in the brain

Received on 14 January 2025; revised on 31 March 2025; accepted on 14 April 2025

and spinal cord.[9] A meta-analysis was undertaken to assess the effectiveness and safety of FTY720 in individuals diagnosed with relapsing–remitting MS. The study showed no significant difference in the occurrence of side effects between the group that received FTY720 and the group that received either a placebo or other disease-modifying therapies. However, it was found that the group that received FTY720 had a significantly lower rate of relapses per year.[10]

FTY720 also has some neuroprotective effects that may slow down the brain atrophy and cognitive decline in MS. FTY720's potent efficacy, oral administration route, and generally excellent safety and tolerability profiles make it a novel treatment option for patients and clinicians. Nonetheless, numerous adverse effects have already been recognized, and the cumulative experience with its use is limited compared to that of other agents. Its novel and complex mechanism of action makes predicting adverse effects difficult.[11] Some of the common adverse events associated with FTY720 are headache, fatigue, diarrhea, back pain, and elevated liver enzymes. FTY720 can also cause serious complications such as bradycardia, infections, macular edema.[12] An increase in liver enzymes has been observed in patients with MS who have been treated with FTY720. There have also been reports of acute liver failure that required liver transplantation, as well as clinically significant liver injury.[13] Due to the frequency of enzyme elevations observed during treatment and subsequent reports of liver injury, the FDA recommends that liver tests to be performed before starting treatment with FTY720. The tests should be repeated at 1, 3, 6, 9, and 12 mo, and thereafter on a routine basis until at least 2 mo after treatment cessation.[14]

This study aims to elucidate the underlying mechanism responsible for the toxicity profile of the drug FTY720, particularly the significant liver injury observed in patients receiving this agent. To achieve this objective, various parameters will be assessed, including cytotoxicity against a representative hepatic cell line, mitochondrial health status, ATP levels, and oxidative stress in response to drug exposure. Furthermore, to advance beyond these in vitro tests, the integration of experimental data obtained here with molecular docking simulations will be employed to establish a hypothesis aimed at precisely identifying the key enzymes responsible for this toxic profile. This advanced computational approach will pave the way for researchers to uncover the mechanism underlying FTY720's toxic action.

Material and methods

Cell culture and treatment conditions

Human liver cancer HepG2 cell line was obtained from American Type Culture Collection (ATCC-HB8065, USA). The cells were cultured in Roswell Park Memorial Institute (RPMI) with fetal bovine serum (FBS, heat inactivated, 10%) and antibiotic (100 U/mL penicillin and 100 μg/mL streptomycin, 1%) with 37 °C and 5% CO_2 conditions.

FTY720 (S)-P was purchased from Cayman Chemical Company (USA) and dissolved in dimethyl sulfoxide (DMSO). HepG2 cells were exposed to FTY720 (S)-P at the range of 0.625–10 μM concentrations for 72 h. Negative control group was indicated as the cells that were exposed to %1 DMSO for all of the assays.

Evaluation of cytotoxicity

The cytotoxic potential of FTY720 (S)-P on HepG2 cells was evaluated by MTT 3-(4,5-dimethylthiazol-2-yl)-2,5-diphenyltetrazolium bromide) assay,[15] lactate dehydrogenase (LDH) activity assay[16] and neutral red uptake (NRU) assay.[17] The cells were exposed to FTY720 (S)-P at the dose range 0.3125–10 μM during 24 h, 48 h and 72 h for the MTT assay and continued with 72 h for all the other cytotoxicity assays. The HepG2 cells were seeded in a 96 well plate at 104/well seeding density and incubated for 24 h. After exposures for all of the assays, the optical densities were measured at 590 nm for MTT assay, 490 nm for LDH assay and 570 nm for NRU assay by microplate reader (Biotek, Epoch, Vermont, USA). Cell viability was expressed as a percentage relative to the control group.

MTT assay

MTT assay is based on the conversion of yellow colour dye salt to purple formazan crystals in viable cells via the activity of mitochondrial succinate dehydrogenase enzyme. The cytotoxicity was evaluated according to this colour change. MTT dye was added to 20 μL/well to the FTY720 (S)-P exposed cells at different concentrations. After 3 h, DMSO was added to dissolve formazan crystals and absorbance was subsequently measured.

LDH assay

LDH activity, was measured using a commercial assay kit (Roche, Germany) following the manufacturer's protocol. LDH is a cytosolic enzyme normally in healthy cells. However, when cytotoxicity occurs, the membrane of the cell becomes damaged, and LDH enzyme releases into the culture media. A linked enzymatic process, in which released LDH enzyme forms pyruvate from lactate via NAD+ reduction to NADH, can be used to measure the amount of extracellular LDH present in the media. A tetrazolium salt (INT) is then reduced by diaphorase using NADH to a red formazan product that has a wavelength of 490 nm. The amount of LDH released into the medium, a sign of cytotoxicity, is closely correlated with the degree of formazan formation.

NRU assay

Through non-ionic passive diffusion, neutral red, a weak cationic dye, builds up in lysosomes and forms electrostatic hydrophobic interactions with the phosphate and/or anionic groups of the lysosomal matrix. By allowing neutral red dye to enter cells, lysosomal integrity serves as a gauge of cell viability in the NRU experiment. The absorbance of the solubilized dye was measured after extracting the dye from the viable cells using an acidified ethanol solution.

Evaluation of mitochondrial damage

The mitochondrial parameters were evaluated by measuring intracellular ATP levels and mitochondrial membrane potential (MMP). The cells were exposed to FTY720 (S)-P at the dose range 0.625–10 μM during 72 h for the assays. The HepG2 cells were seeded in a 24 well plate at 5×10^4/well seeding density for the ATP assay; 25 cm^2 flasks at $2{,}5 \times 10^5$ seeding density for the MMP assay and incubated for 24 h.

ATP content determination

The intracellular ATP levels were quantified using a commercially available Luminescent ATP Detection Assay Kit (Abcam, UK), following the manufacturer's protocol. Luminescence was measured using a microplate reader (BioTek Synergy H1, Epoch, Germany), and the ATP concentration was determined based on a standard curve. The protein concentration was assessed using a Pierce BCA protein assay kit (Thermo Scientific, United States). The ATP concentration was normalized to the protein content, and the results were expressed relative to the control group.

Determination of MMP

The MMP was evaluated using the JC-1 fluorescent dye (Invitrogen, USA). JC-1 is a cationic dye that accumulates in healthy mitochondria, forming red fluorescent aggregates. However, when MMP is lost, JC-1 can't accumulate as aggregates, becomes in a monomeric form and shows green fluorescence.[18] Fluorescence intensity was measured with flow cytometer (ACEA NovoCyte) in FL-1 (FITC) and FL-2 (PE) channels. The results were analysed using Novoexpress software (ACEA, CA, USA).

Determination of oxidative stress

The oxidative stress parameters were evaluated by cellular ROS generation and mitochondrial superoxide (mtSOD) production. The cells were seeded in a 6 well plate at $2{,}5x10^5$/well seeding density for the assays. Also, the antioxidant response of HepG2 cells after FTY720-P exposure was evaluated by measuring total SOD (t-SOD) enzyme activity, catalase (CAT) enzyme activity, and glutathione (GSH) levels. The cells were seeded in a 25 cm^2 flasks at $1x10^6$ seeding density for all the assays and incubated for 24 h.

ROS production level

Intracellular ROS production was measured using the 2′,7′-dichlorodihydrofluorescein-diacetate (H_2DCF-DA) fluorescent dye following 72 h exposure to FTY720 (S)-P. After H_2DCF-DA penetrates the cell membrane, cellular esterase deacetylate H_2DCF-DA to produce the non-fluorescent molecule H_2DCF. This molecule is then oxidized to produce the green fluorescent DCF by intracellular ROS in the medium. The fluorescence intensity is related to diffusing fluorescence and increased ROS levels.[19] Flow cytometric analysis was carried out with ACEA flow cytometer in FITC channel (excitation at 488 nm; emission at 530 nm). Data were analysed using Novoexpress software, and the results were expressed as the percentage of median fluorescence intensity. This was calculated by dividing the median fluorescence intensity (MFI) of the treated samples by the MFI of the control and multiplying by 100.

Determination of mitochondrial superoxide

Mitochondrial superoxide (mtSOD) production was assessed using the MitoSox Red fluorescent dye (Invitrogen, Massachusetts, USA), following the manufacturer's protocol. The cells were exposed to H_2O_2 (500 μM) for 30 min as a positive control. Fluorescence intensity was measured using ACEA flow cytometer. The experimental data were analysed using Novoexpress software. Results were expressed as a percentage of MFI, calculated by dividing the MFI of the treated samples by the MFI of the control and multiplying by 100. MFI levels of the treatment groups were normalized to the control group.

Determination of T-SOD activity

Total SOD (t-SOD) enzyme activity was determined using a commercially available Total Superoxide Dismutase (T-SOD) Activity Assay Kit (WST-1 Method) (Elabscience, USA) following the manufacturer's protocol. The absorbance was measured at 450 nm using a microplate reader (Biotek, Epoch, Vermont, USA). Result was expressed as U/mg protein. The protein content was measured with the Pierce BCA protein assay kit (Thermo Scientific, USA).

Determination of CAT activity

Catalase (CAT) enzyme activity was determined using a commercially available Catalase (CAT) Activity Assay Kit (Elabscience, USA) following the manufacturer's protocol. The catalytic decomposition of hydrogen peroxide (H_2O_2) by CAT can be expeditiously inhibited by ammonium molybdate. The remaining H_2O_2 undergoes a reaction with ammonium molybdate resulting in the formation of a yellow-coloured complex. The absorbance was measured at 405 nm using a microplate reader (Biotek, Epoch, Vermont, USA) and the results were expressed as U/mg protein. The protein content was measured with the Pierce BCA protein assay kit (ThermoFisher Scientific, USA).

Determination of GSH levels

Glutathione (GSH) levels were determined using the method described by Beutler et al., (1963)[20] which is based on the reaction of 5,5′-dithiobis-2-nitrobenzoic acid (DTNB) with free sulfhydryl groups, producing a yellow-coloured 2-nitro-5-mercaptobenzoic acid compound. The absorbance was measured at 412 nm using a microplate reader (BioTek Synergy H1). The protein concentrations were determined using the BCA Protein Assay kit (ThermoFisher Scientific, USA), and results were reported as ng/mg of protein.

Molecular docking study

Molecular docking studies are valuable computational tools designed to investigate interaction profiles, predict fitting poses, and visualize the physical forces established between a receptor and its docked ligands. These interactions are quantified by a docking score, where more negative values indicate stronger binding and a more compatible ligand-protein complex. Additionally, molecular docking can effectively guide researchers before proceeding to in vitro experimental stages, particularly in studies aiming to elucidate unclear or complex drug mechanisms of action. Herein, as the hepatotoxic profile of FTY720 (S)-P is hypothesized to primarily result from its interaction with sirtuins (SIRTs), particularly SIRT3 and SIRT5, a molecular docking study was conducted to evaluate the validity and precision of this hypothesis. The study comprised three main stages: ligand modelling and preparation, protein selection and preparation, and receptor grid generation.

In the first stage, the employed ligands were modelled using the Maestro Graphical User Interface, part of the Schrödinger Suite (version 14.2). Ligand preparation followed, generating all possible ionization states at a physiological pH of 7.0 ± 2.0 and identifying relevant conformations. To ensure suitability for docking, the ligands were then energy-minimized using the OPLS2005 force field.[21,22]

To initiate the protein preparation process, the crude crystallographic structures of the target enzymes, SIRT3 and SIRT5, were retrieved from the Protein Data Bank (https://www.rcsb.org/). The human SIRT3 structure (PDB ID: 4JSR) with a resolution of 1.70 Å, complexed with the ELT inhibitor, was selected to represent the SIRT3 protein. Similarly, the human crystal structure (PDB ID: 5XHS), resolved at 2.19 Å and complexed with a fluorogenic small-molecule substrate (SuBKA), was utilized for SIRT5. Subsequently, the retrieved protein structures were prepared to be reliable for molecular docking studies using the Schrödinger Maestro Protein Preparation Wizard.[23] This stage involved several refinement steps, including adding hydrogen atoms, rebuilding missing side chains, deleting water molecules within 3 Å of heteroatoms, assigning bond orders and charge states to the protein's functional groups, and finalizing the process by optimizing and minimizing the protein crystal structure using the OPLS_2005 force field.

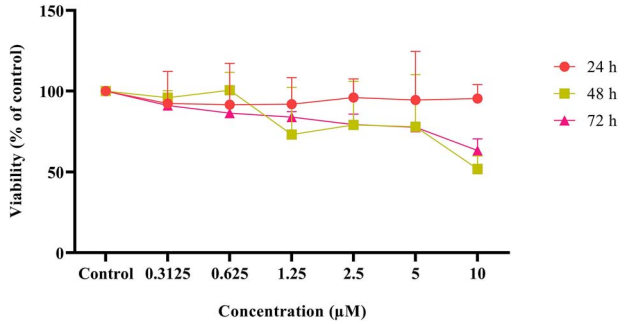

Fig 1. Effects of cytotoxicity observed with FTY720 (S)-P exposure on HepG2 cells after 24–48 and 72 h treatment. The cells were treated with 0.3125–10 μM concentrations.

Afterward, to enhance the precision of the docking study by directing the docked substrates to the correct binding site, a receptor grid was generated with dimensions of 10 Å × 10 Å × 10 Å, based on the native ligands of the subject proteins.

Upon completing the aforementioned three main steps, the molecular docking simulation was performed using the Extra Precision (XP) Glide docking mode integrated into the Schrödinger-Maestro software (version 14.2), employing the default parameters.[24] The docking pose for each ligand-protein complex was visualized using the Maestro Schrödinger interface. Additionally, a thorough analysis of the interaction profile for each complex was conducted using the Protein-Ligand Interaction Profiler (PLIP) server.[25]

Statistical analysis

All results were normalized to the control group. Statistical analysis was conducted using Graphpad Prism 9 (GraphPad Software Inc, CA, USA). Differences were assessed with one-way ANOVA followed by the post-hoc Tukey test. Results are presented as mean ± standard deviation (SD). $^{*}P < 0.05$, $^{**}P < 0.01$ were considered statistically significant.

Results

Cytotoxicity

The mortality rate observed at the highest exposure (10 μM) was 36.74% ± 3.50% for 72 h exposure. Comparison of different exposure times (24–72 h) revealed that the dose-dependent increase in cell death also escalated with longer exposure periods. However, despite long-term exposure, higher concentrations could not be used to fully characterize the cytotoxicity profile of FTY720 (S)-P or determine the half-maximal inhibitory concentration (IC_{50}) value, as the experimental conditions did not allow this. The linear dose–response relationship and cytotoxicity profile were most evident following 72 h of FTY720 (S)-P treatment in the HepG2 cell line (Fig. 1). Then, the cytotoxic potential of FTY720 (S)-P was compared with three cytotoxicity assays, MTT, LDH, and NRU (Fig. 2).

The cytotoxic potential of FTY720 (S)-P on the HepG2 cell line was evaluated using three cytotoxicity assays: MTT, LDH, and NRU. The MTT assay demonstrated a significant >20% reduction in HepG2 cell viability after 72 h of 5 and 10 μM FTY720 (S)-P treatment. The LDH assay showed that 10 μM exposure reduced cell viability to 95.48%, and this decrease was statistically significant compared to the control ($P > 0.05$). The NRU assay revealed a cell death rate of 35.03% ± 7.3% at the 10 μM concentration.

Mitochondrial damage

Intracellular ATP levels exhibited a dose-dependent decrease, with a statistically significant ($^{*}P < 0.05$) 56.89 ± 2.93% reduction observed at the highest concentration compared to the control, almost reduced the level of H_2O_2 (Fig. 3).

The changes in the MMP of HepG2 cells were examined following exposure to FTY720 (S)-P. At lower doses, a significant decline was observed compared to the control (16.60 and 25.48% for 0.625 and 1.25 μM, respectively; $P < 0.001$). At higher doses, the change was less pronounced, with a statistically significant alteration observed only at the 10 μM concentration ($P < 0.01$) (Fig. 4).

Oxidative stress

The FTY720 (S)-P-induced oxidative damage was evaluated by assessing cellular ROS and mt-ROS levels. Cellular ROS levels showed a statistically significant 1.75-fold increase ($P < 0.01$) compared to the control, but only at the 1.25 μM concentration. In contrast, mt-ROS levels exhibited a dose-independent pattern, with a 0.7-fold decrease ($P < 0.01$) at the 1.25 μM concentration relative to the control (Fig. 5).

The changes in the antioxidant defence system observed with FTY720 (S)-P exposure were evaluated through the levels of CAT, t-SOD, and GSH. The CAT enzyme level showed an increase at the 0.625 and 5 μM exposure concentrations with a 4.5-fold rise at the lowest exposure concentration, compared to the control ($P < 0.01$). However, GSH levels exhibited a significant 1.25-fold decrease at the highest concentration of 10 μM. On the other hand, in t-SOD levels, first there was a significant decrease in 2.5 μM but in 5 μM exposure concentration, there was a significant increase compared to the control ($P < 0.05$) (Fig. Fig. 6).

Molecular docking study

Chemoinformatic tools, such as molecular docking simulations, are considered trustworthy for assessing ligands affinities and visualizing their binding poses and interaction profiles within the target protein's binding site. The tools, validated through extensive research and practical application, have proven their value in drug discovery and development, as well as in elucidating the mechanisms of action of drugs and their associated side effects. Herein, the investigation into the underlying causes of the hepatotoxic side effects associated with FTY720 (S)-P identified several contributing factors, including mitochondrial damage, reduced ATP levels, and increased oxidative stress. Based on molecular docking studies, the primary mechanism behind these toxic effects is hypothesized to be the inhibition of two critical enzymes, SIRT3 and SIRT5.

Initially, the reliability of the retrieved X-ray crystallographic proteins (PDB ID: 4JSR for SIRT3 and PDB ID: 5XHS for SIRT5), the software employed, and the docking protocol was assessed through a superposition check. This evaluation involved superposing the native ligand of each X-ray crystallographic protein over its respective docked conformation, followed by calculating the root mean square deviation (RMSD) value. An optimal RMSD value is considered to be below 2 Å, indicating a reliable docking protocol. As demonstrated in Fig. 7, superimposing the crystal conformations of ETL and SuBKA substrates, which serve as native ligands for SIRT3 and SIRT5, respectively, onto their respective docked conformations resulted in RMSD values of 0.426 and 1.220 Å. These values highlight the reliability and accuracy of the retrieved crystallographic proteins, the software used, and the docking protocol.

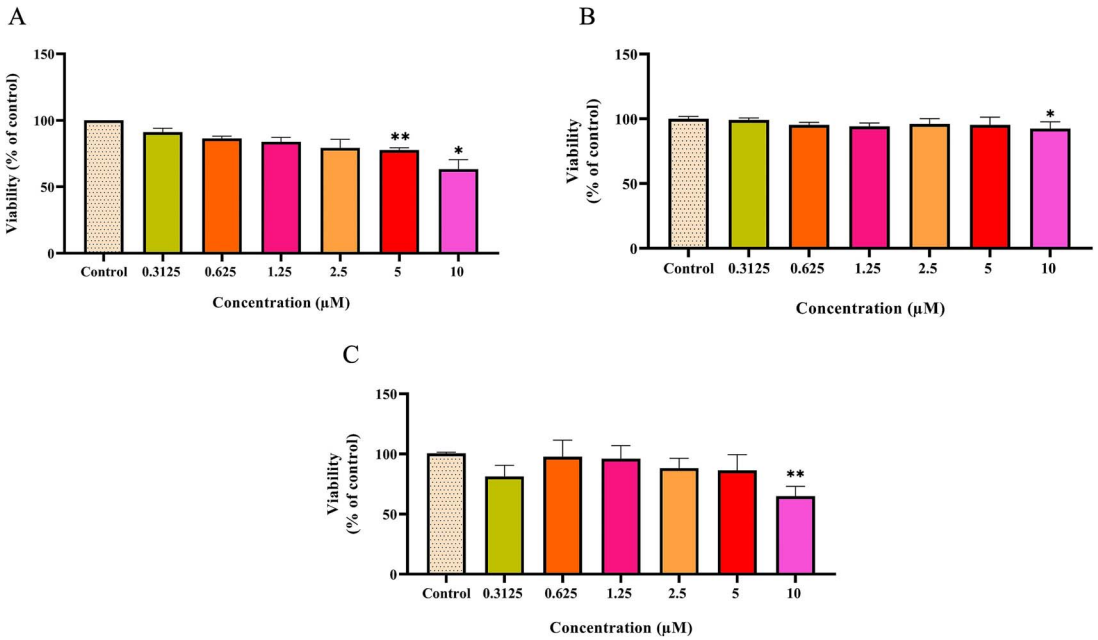

Fig 2. Effects of FTY720-S(P) (0.3125–10 μM) on cell viability by A) MTT, B) LDH and C) NRU assays in HepG2 cells after 72 h treatments. The cells were treated with 0.3125–10 μM concentrations. Data are expressed as mean ± SD, *$P < 0.05$ and **$P < 0.01$ versus the control group.

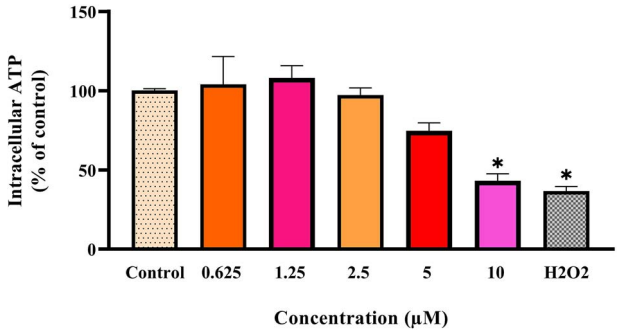

Fig 3. Changes in the ATP content observed with FTY720 (S)-P exposure on HepG2 cells after 72 h treatment. The cells were treated with 0.625–10 μM concentrations. Data are expressed as mean ± SD, *$P < 0.05$ versus the control group.

Interrogating the docked complex of FTY720 (S)-P within the binding sites of both SIRT3 and SIRT5 reveals the formation of optimal binding profiles, characterized by significant interactions and well-aligned poses, as depicted in Fig. 8 and Table 1. These findings suggest that FTY720 (S)-P acts as a potent ligand for both targets. Specifically, in the SIRT3 complex, the phosphate group of FTY720 (S)-P establishes two hydrogen bonds with the ALA146 and THR320 residues. Additionally, it forms two salt-bridge hydrogen bonds with fully ionized surrounding amino acids, ARG158 and ASP156, which play a crucial role in enhancing the ligand's affinity for the target binding site. This robust interaction profile is further reinforced by the hydrophobic interactions facilitated by the lipophilic nature of the phenyl-aliphatic chain moiety, engaging with the surrounding residues PHE180, HIS248, PHE294, and LEU298. For the SIRT5 complex, the docking of FTY720 (S)-P reveals the formation of three significant hydrogen bonds with ARG71, VAL221, and TYR102. The positively charged ARG105 residue establishes both salt bridges and water-mediated interactions with FTY720 (S)-P. Additionally, the interaction analysis highlights hydrophobic interactions involving lipophilic residues such as VAL221, PHE223, LEU227, and LEU232. These exceptional interaction profiles are reflected in the highly favourable docking scores of −7.07 and − 7.64 kcal/mol for the SIRT3 and SIRT5 complexes, respectively.

Discussion

The aim of our study was to examine the toxic effects of FTY720 (S)-P, the phosphorylated active form of FTY720, using the HepG2 cell line. On a cellular scale, toxic effects can eventually result in organ-specific injury, including liver damage and hepatotoxicity. Elevated liver enzymes, acute liver failure that requires liver transplantation, and clinically significant liver injury are main indicators of hepatotoxicity.[26,27] Therefore, the HepG2 human hepatocellular cell line was deemed suitable for investigating the adverse effects of FTY720 (S)-P in this study.

Since the toxicity mechanisms caused by FTY720 (S)-P, particularly in the liver where FTY720 is phosphorylated, have not been sufficiently investigated and there is a lack of studies on this topic in the literature, the planned study will focus on mitochondria and oxidative stress aiming to clarify the underlying mechanisms of FTY720 (S)-P-induced hepatotoxicity.

The liver is well-known as the primary organ affected by toxicity since it plays such a crucial role in the metabolism and detoxification of xenobiotic, both pharmaceutical and non- pharmaceutical.[28] Mitochondrial dysfunction, loss of mitochondrial membrane potential, reduction in ATP generation, release of ROS, and DNA damage are all examples of mitochondrial damage that contribute to liver injury.[29]

Based on the findings of our current study, FTY720 (S)-P does not show significant cytotoxicity in the HepG2 cell line. Unlike FTY720 (S)-P, non-phosphorylated form of FTY720 exerts cytotoxicity in several cancer cell lines, HepG2 (IC_{50}: 13 μM), Huh-7 (IC_{50}: 12 μM) and Hep3B (IC_{50}: 14 μM) with varying p53 status, as well as one non-tumorigenic immortalized liver cell line MIHA (IC_{50}: 60 μM). The reported antitumor activity of FTY720 is attributed to ROS production, Akt activation, and subsequent caspase-3-dependent apoptotic effects.[8,30,31] Hagihara et al. (2013)[32] showed

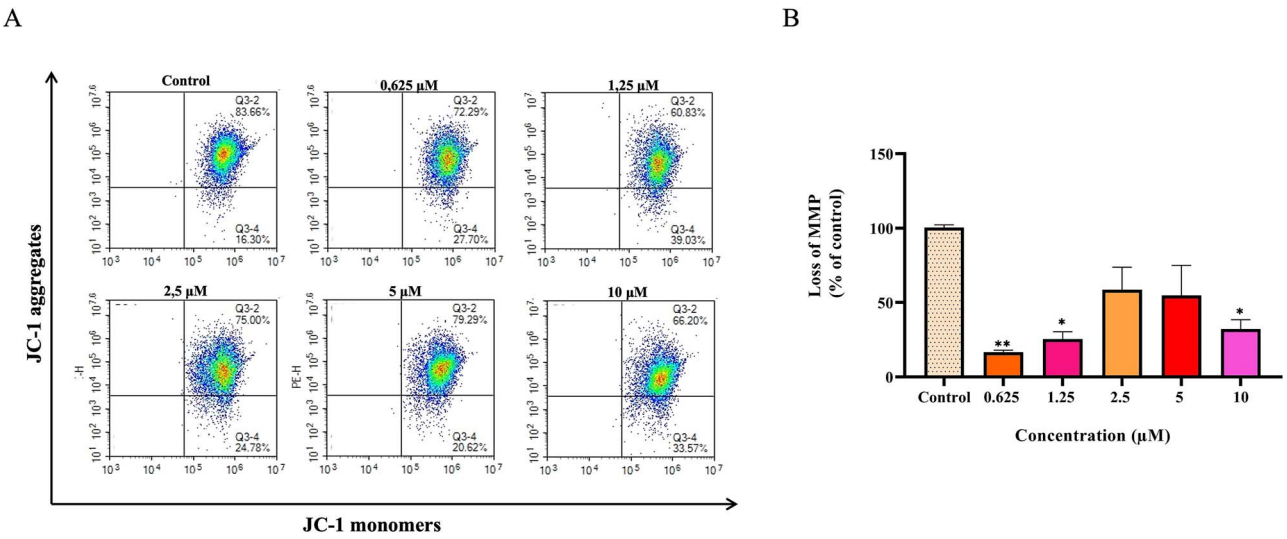

Fig 4. Changes in mitochondrial membrane potential (MMP) observed with FTY720 (S)-P exposure on HepG2 cells after 72 h treatment. A) Quadrants of JC-1 aggregates (PE channel) and monomers (FITC channel), B) MMP levels. The cells were treated with 0.625–10 μM concentrations. Data are expressed as mean ± SD, *$P < 0.05$ and **$P < 0.01$ versus the control group.

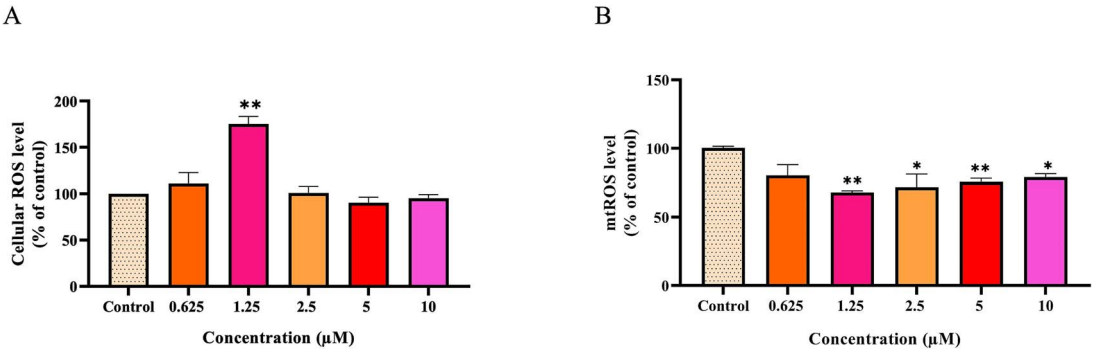

Fig 5. Oxidative stress production observed with FTY720 (S)-P exposure on HepG2 cells after 72 h treatment. A) Cellular ROS production, B) mitochondrial ROS production. The cells were treated with 0,625–10 μM concentrations. Data are expressed as mean ± SD, *$P < 0.05$, **$P < 0.01$ versus the control group.

Table 1. The Interaction profiles and docking scores of FTY720 (S)-P within the binding pocket of the SIRT3 (PDB ID: 4JSR) and SIRT5 (PDB ID: 5XHS) proteins.

Target	Hydrogen bonds	Salt bridges	Water bridges	Hydrophobic	Docking Score (kcal/mol)
SIRT3 (4JSR)	ALA146, THR320	ARG158, ASP156	-	PHE180, HIS248, PHE294, LEU298	−7.17
SIRT5 (5XHS)	ARG71, VAL221, TYR102	ARG105	ARG105	VAL221, PHE223, LEU227, LEU232	−7.75

that FTY720, but not FTY720 (S)-P, induced cytotoxicity in fission yeast *(Schizosaccharomyces pombe)*. Studies provided evidence that FTY720 (S)-P does not exhibit any notable cytotoxic effects. In parallel with the current literature, we found that in our study, FTY720 (S)-P exposure led to dose- and time-dependent decreases in cell viability, with the highest exposure concentration (10 μM) resulting in a cell death rate of ≤36.74%. The finding further supports the notion that the cytotoxic impact of FTY720 involves mechanisms that are independent of phosphorylation and S1P signalling. Additionally, accumulating evidence demonstrates that the FTY720-induced cytotoxicity in various cancer cells is dependent on the production of ROS.[8]

When the potential cytotoxicity of FTY720 (S)-P was compared across three different assays, a statistically significant reduction was observed at the highest concentration consistently across all tests. According to the LDH assay, which indicates cell membrane damage and cell death, exposure to ≤10 μM FTY720 (S)-P resulted in cell death rates close to the control. The NRU assay, a marker of lysosomal damage, revealed a dose-dependent potential for FTY720 (S)-P to induce lysosomal injury. Additionally, the MTT assay, which evaluates mitochondrial damage and cell proliferation, showed a significant decrease in cell viability at high concentrations compared to the control. In this context, the effect of FTY720 (S)-P on the viability of HepG2 cells can be ranked as LDH < NRU < MTT.

Zhang et al. (2010)[33] demonstrated that FTY720 exhibited strong, dose- and time-dependent cytotoxic effects in human ovarian cancer cells, including those resistant to the commonly

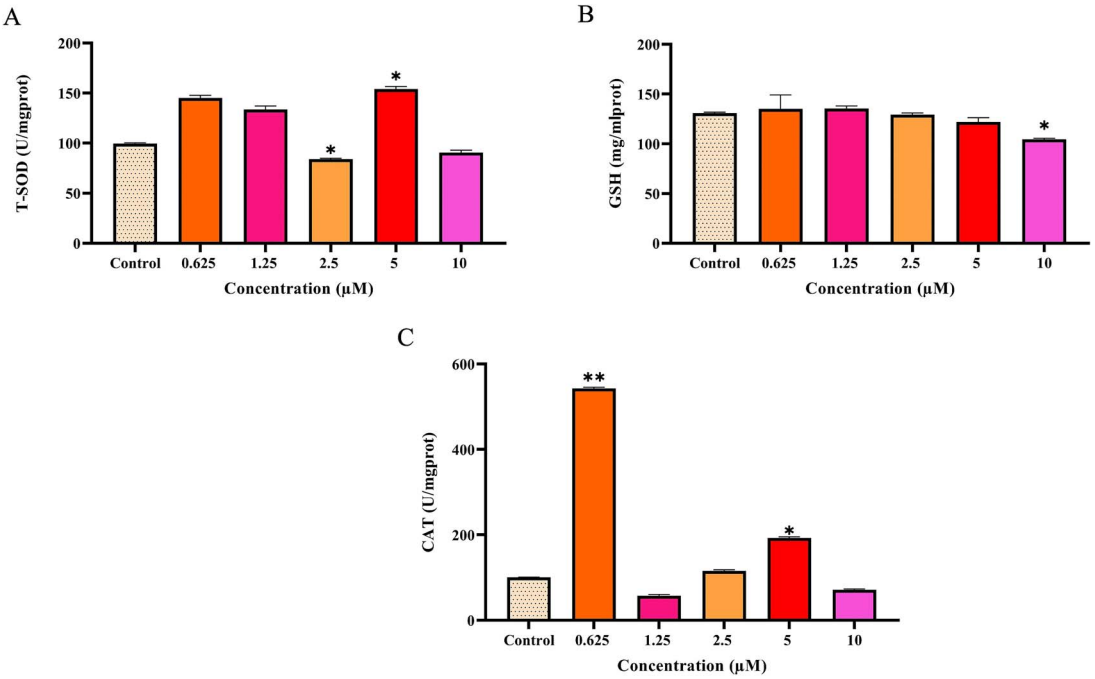

Fig. 6. Changes in antioxidant enzyme levels observed with FTY720 (S)-P exposure on HepG2 cells after 72 h treatment. A) Total superoxide dismutase (T-SOD), B) glutathione (GSH), (C) catalase (CAT). The cells were treated with 0.625–10 μM concentrations. Data are expressed as mean ± SD, *$P < 0.05$, **$P < 0.01$ versus the control group.

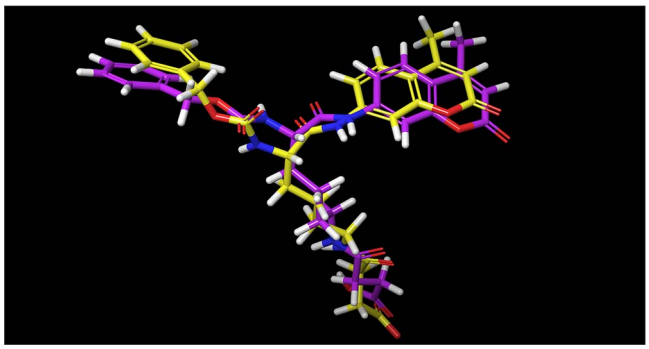

Fig 7. Superposition of the native ligand in its crystallized conformation with its respective docked conformation for SIRT3 (PDB ID: 4JSR) and SIRT5 (PDB ID: 5XHS) enzymes, showing RMSD values of 0.426 Å and 1.22 Å, respectively.

prescribed chemotherapeutic agent cisplatin. The researchers emphasized that FTY720-induced autophagy may play a protective role against its own cytotoxic effects, and that targeting autophagy could enhance the anticancer potential of FTY720, suggesting this data could be evaluated for further development of FTY720 as a treatment for ovarian cancer. Ahmed et al. (2015)[34] evaluated the effects of combined FTY720 and the multi-kinase inhibitor sorafenib on hepatocellular cell lines Huh7 and HepG2. They reported that the decrease in cell viability observed with increasing doses of sorafenib was enhanced by the synergistic effect of FTY720. The researchers underscored that hepatocellular cells are sensitive to the cytotoxic effects of FTY720, and that the impact of the sorafenib and FTY720 combination therapy warrants further investigation.

According to Hagihara et al. (2014),[35] FTY720 was identified as a ROS-inducing compound that stimulates the Spc1/Sty1 MAPK signalling pathway in fission yeast *(Schizosaccharomyces pombe)*. The researchers demonstrated that the accumulation of ROS following FTY720 treatment, due to impaired Sty1 MAPK function, led to the suppression of antioxidant enzymes like catalase and glutathione gene expression. However, FTY720 (S)-P was reported to not induce cytotoxicity. Other studies have shown that FTY720 (S)-P does not exhibit significant cytotoxic effects, further confirming that the cytotoxic activity of FTY720 involves mechanisms independent of phosphorylation and S1P signalling.[8]

Despite its low cytotoxicity, ATP levels were observed to be downregulated starting at 1.25 μM. ATP depletion could indicate cellular stress. Since oxidative phosphorylation in the mitochondria is responsible for ATP synthesis, assessing ROS levels might help explain the reduction in ATP levels seen after FTY720 (S)-P treatment. Optimal levels of ROS play a crucial role in cellular processes and signalling pathways that promote cell viability. However, an excessive accumulation of ROS can induce cell death by several mechanisms, including as apoptosis, necrosis and autophagy.[36]

Hepatocytes have high energy demands. Hepatocyte dysfunctions are exacerbated by damage to the ATP-generating mitochondria. Necrosis rather than apoptosis results from ATP depletion throughout the cell, which is prevented by the opening of holes in the mitochondrial inner membrane via permeability transition.[29,37] In our study, the intracellular ATP levels in HepG2 cells exhibited a dose-dependent decrease upon exposure to FTY720 (S)-P with a 48.74% reduction observed at the highest concentration (10 μM). Consistent with this finding, the mitochondrial membrane potential levels in HepG2 cells displayed a concentration-independent decrease with FTY720 (S)-P treatment. While lower concentrations (0.625 and 1.25 μM) led to a significant reduction in MMP levels (16.60 and 25.48%, respectively; $P < 0.001$), higher doses showed a less pronounced decrease, with the change not reaching statistical significance. However, the alteration observed at the highest concentration (10 μM) was statistically significant (32.26% decrease, $P < 0.01$).

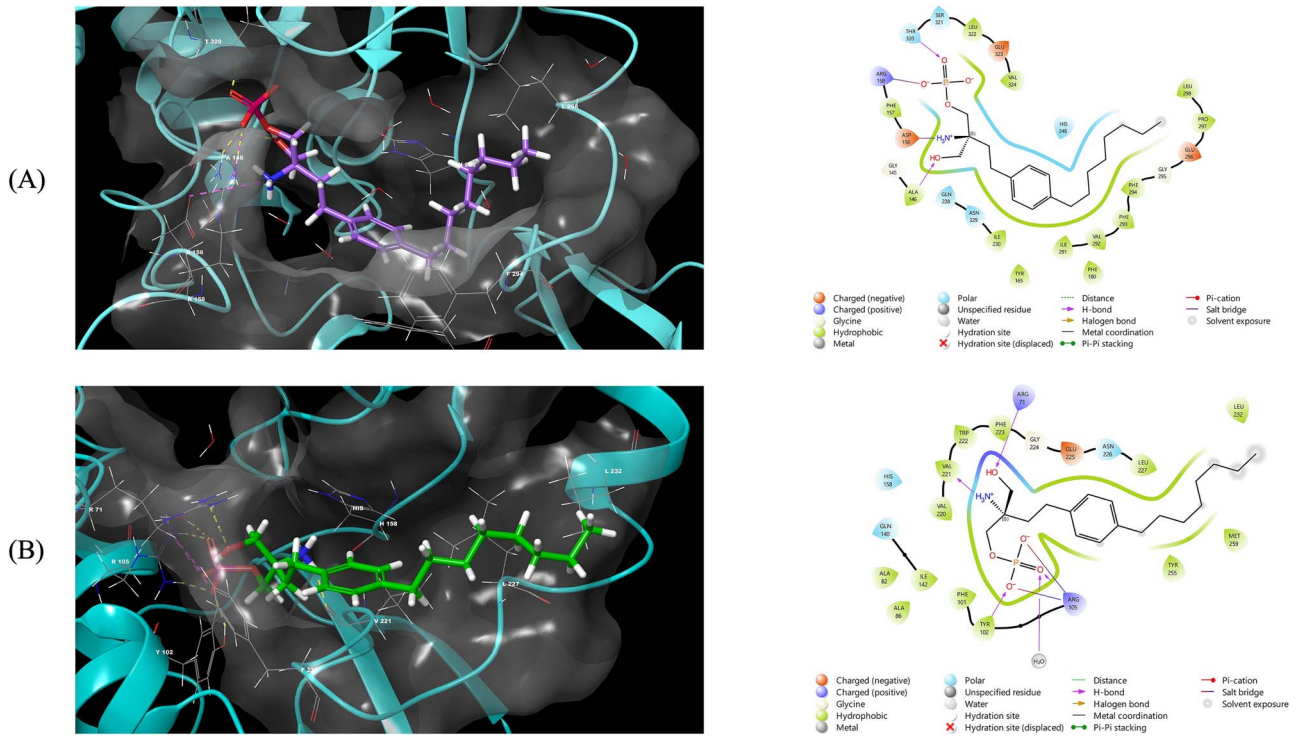

Fig 8. Molecular docking of FTY720 (S)-P depicted as 2D and 3D simulations within the binding sites of human SIRT3 (A) and SIRT5 (B), utilizing the X-ray crystallographic structures with PDB codes 4JSR and 5XHS, respectively.

One of the key mechanisms of drug-induced liver injury is assumed to be mitochondrial dysfunction.[37] Our study found that FTY720 (S)-P induced oxidative damage at both the cellular and mitochondrial levels. The oxidative potential of FTY720 (S)-P exposure was evaluated through changes in cellular ROS and mt-ROS levels, as well as the antioxidant defence system. Cellular ROS levels showed a significant increase (1.75-fold; $P < 0.01$) only at the 1.25 μM concentration, while mt-ROS levels exhibited concentration-independent variations, with a significant decrease (0.7-fold; $P < 0.001$) observed only at 1.25 μM. Similarly, GSH levels decreased significantly ($P < 0.05$) only at the highest exposure concentration. CAT enzyme levels increased significantly (4.5-fold; $P < 0.01$) at the lowest exposure concentration of 0.625 μM, whereas T-SOD levels showed a significant decline ($P < 0.05$) across a wide range of concentrations (1,25–5 μM).

Gil et al. (2020)[38] carried out a study to investigate the molecular mechanisms underlying the protective effects of FTY720 (S)-P against VitK3-induced oxidative damage. The study examined enzymes related to $O_2 -\bullet$ metabolism and found an increase in mitochondrial SOD activity (%77,3) in VitK3-treated neurons compared to controls, which was not compensated by changes in CAT or GPX activities, suggesting that VitK3-triggered oxidative stress may be mitochondrial in nature. It was emphasized that one of the inducers of SOD expression, a mitochondrial enzyme that promotes H_2O_2 formation, is the increase in $O_2 -\bullet$. Additionally, the study reported that the decrease in SOD activity in the presence of FTY720 (S)-P compared to control indicates the protective effect of FTY720 (S)-P on mitochondrial functions.

A study by Martín-Montañez et al. (2019)[39] examined the antioxidant characteristics of FTY720 (S)-P in a model of VitK3-induced mitochondrial oxidative injury, utilizing the SN4741 dopaminergic cell line derived from the mouse substantia nigra. The results showed that VitK3 incubation led to an increase in cellular mt-ROS levels compared to control, but this effect was reversed in the presence of FTY720 (S)-P. The same study found that the dramatic decrease in MMP observed in the control was largely restored in the presence of FTY720 (S)-P. The researchers suggested that the decrease in total thiols in the presence of FTY720 (S)-P could lead to the dysfunction of GST, GPX4, and/or other key enzymes involved in the detoxification of ROS-induced products, which may result in cell death involving apoptosis, ferroptosis, and necrosis, as observed in certain neurodegenerative diseases such as MS.

Molecular docking simulation is a cornerstone of cheminformatics studies, playing a pivotal role in accelerating drug discovery and development processes. This powerful computational technique is employed to evaluate the activity of chemical agents against their target proteins by analysing their interaction profiles and binding geometry within the protein's active site. Furthermore, molecular docking is instrumental in elucidating the mechanisms of action of drugs, providing insights into their side effects. By facilitating targeted drug research, this approach helps streamline the drug development process, saving both time and resources while contributing to enhanced drug safety and efficacy.[40] Herein, the hepatotoxicity and overall toxic profile observed for FTY720 (S)-P have been experimentally attributed to mitochondrial dysfunction, diminished ATP production, increased oxidative stress, and its dose- and time-dependent cytotoxicity. Based on molecular docking analyses and literature evidence, this toxic profile appears to originate primarily from the inhibition of sirtuin enzymes (SIRTs), specifically SIRT3 and SIRT5.[41,42]

These enzymes are critical in regulating protein activity, serving as key post-translational modulators through nicotinamide adenine dinucleotide (NAD+)-dependent lysine residue deacetylation mechanisms in response to various stressors and nutrient fluctuations.[43] Consequently, dysregulation of SIRTs is implicated

in metabolic disorders and aging-related diseases.[44] SIRTs also serve as fundamental mediators in cellular stress responses through various mechanisms, including the regulation of energy metabolism proteins, support of mitochondrial functionality, and deacetylation of antioxidant enzymes.[45] In particular, SIRT3 functions as a direct activator of various proteins within the mitochondrial network, leveraging its capacity to regulate stress responses, lipid metabolism, oxidative phosphorylation, and the tricarboxylic acid (TCA) cycle.[46,47] Conversely, the presence of TYR102 and ARG105 residues within the binding site of SIRT5, instead of GLY202 and LYS205 in the SIRT3 protein, plays a pivotal role in modulating the mitochondrial urea cycle. This is attributed to the exceptional ability of these critical residues to facilitate the desuccinylation or demalonylation of SIRT5's substrates.[48,49] Moreover, mitochondrial metabolism is proposed to be influenced by additional SIRT5-associated mechanisms, particularly through the succinylation of both succinate dehydrogenase and the pyruvate dehydrogenase complex.[50]

The hypothesis that the hepatotoxic profile of FTY720 (S)-P is linked to the targeting of SIRT enzymes is strongly supported by the critical roles these enzymes play in maintaining mitochondrial health and their close association with the normal state of hepatic cells, as previously mentioned. This theory is further reinforced by the high abundance of SIRT proteins in hepatic cells, highlighting the strong correlation between SIRT inhibition, mitochondrial dysfunction, and liver injury[51,52] as summarized in Scheme 1.

The analysis of the binding mode of FTY720 (S)-P within the binding pockets of both SIRT3 and SIRT5 proteins provides strong support for the proposed hypothesis. The results reveal significant docking scores around −7 kcal/mol, indicative of robust physical interactions with surrounding residues and an optimal fit within the binding sites, as illustrated in Fig. 8. Furthermore, the binding profiles of FTY720 (S)-P closely resemble those observed for previously identified potent SIRT3 and SIRT5 inhibitors, such as fusaric acid and SuBKA, which exhibit SIRT inhibition potency in the nanomolar range. The findings further substantiate the role of FTY720 (S)-P as an effective ligand targeting SIRT3 and SIRT5.[53–56]

These findings may be valuable for further experimental evaluation of the drug's potential effects on the SIRT family, as well as its role in drug-induced mitochondrial toxicity. Additionally, investigating liver mitochondria following FTY720 (S)-P treatment in vivo could provide a promising approach for understanding its mechanisms of action and toxicity. Despite the well-documented physiological and therapeutic effects of this compound, the complex mechanism of action of FTY720 (S)-P remains elusive. While FTY720 has immunosuppressive effects and is used to treat multiple myeloma, the disease still poses significant management challenges, highlighting the urgent need for more effective therapeutic protocols. Therefore, in addition to assessing the safety of current agents like FTY720, there is a clear necessity for the development of new drug molecules. Studies exploring this topic are expected to provide valuable contributions to researchers and the literature.

Conclusion

In conclusion, this study provides valuable insights into the hepatotoxic mechanisms of FTY720 (S)-P, the active metabolite of FTY720. The drug exhibited dose- and time-dependent effects on cell viability, ATP levels, mitochondrial membrane potential, and oxidative stress, highlighting the multifaceted nature of its toxicity. By combining in vitro experimental findings with molecular docking simulations, the study identifies the potential interaction of FTY720 (S)-P with sirtuin proteins, particularly SIRT3 and SIRT5, as a critical factor contributing to its complex toxic profile, especially the pronounced hepatotoxicity. These results mark a significant advancement in understanding the molecular basis of FTY720 (S)-P-induced liver damage and establish a foundation for future research to devise strategies aimed at minimizing its adverse effects while maintaining its therapeutic efficacy.

Acknowledgments

This study was supported by Istanbul University Scientific Research Projects Unit (Project number: TDK-2022-38536).

Authors' contributions

A.B.: Investigation, Methodology, Performed the experiments, Interpreted the results, Writing - Original Draft, Z.Ş.: Investigation, Performed the experiments, Interpreted the results, Writing-Original draft, M.T.Q.: Visualization, Software, Interpreted the results, Writing - Original Draft, G.Ö.: Conceptualization, Methodology, Project administration, Supervision, Interpreted the results, Writing. All authors reviewed the manuscript.

Supplementary material

Supplementary material is available at *Toxicology Research* online

Funding

None declared.

Conflicts of interest

The authors declare that they have no known competing financial interests or personal relationships that could have appeared to influence the work reported in this paper.

There are no conflicts of interest to declare.

References

1. Hauser SL, Cree BAC. Treatment of multiple sclerosis: a review. *Am J Med*. 2020:133:1380–1390.e2. https://doi.org/10.1016/j.amjmed.2020.05.049
2. National Multiple Sclerosis Society. *Types of MS*. New York, USA: National Multiple Sclerosis Society, Retrieved 2023 April 28, from https://www.nationalmssociety.org/What-is-MS/Types-of-MS/Relapsing-remitting-MS
3. Ingwersen J et al. Fingolimod in multiple sclerosis: mechanisms of action and clinical efficacy. *Clin Immunol*. 2012:142:15–24. https://doi.org/10.1016/j.clim.2011.05.005
4. Volpi C et al. Preclinical discovery and development of fingolimod for the treatment of multiple sclerosis. *Expert Opin Drug Discov*. 2019:14:1199–1212. https://doi.org/10.1080/17460441.2019.1646244
5. Chiba K. Discovery of fingolimod based on the chemical modification of a natural product from the fungus, Isaria sinclairii. *J Antibiot*. 2020:73:666–678. https://doi.org/10.1038/s41429-020-0351-0
6. Chun J, Hartung HP. Mechanism of action of oral fingolimod (FTY720) in multiple sclerosis. *Clin Neuropharmacol*. 2010:33:91–101. https://doi.org/10.1097/WNF.0b013e3181cbf825

7. LiverTox. *Clinical and research information on drug-induced liver injury [internet]*. Bethesda (MD): National Institute of Diabetes and Digestive and Kidney Diseases; 2012. Fingolimod. [Updated 2021 Aug 10]. Available from: https://www.ncbi.nlm.nih.gov/books/NBK548384/
8. Takasaki T, Hagihara K, Satoh R, Sugiura R. More than just an immunosuppressant: the emerging role of FTY720 as a novel inducer of ROS and apoptosis. *Oxidative Med Cell Longev*. 2018:2018:4397159. https://doi.org/10.1155/2018/4397159
9. Kappos L et al. A placebo-controlled trial of oral fingolimod in relapsing multiple sclerosis. *N Engl J Med*. 2010:362:387–401. https://doi.org/10.1056/NEJMoa0909494
10. Yang T et al. The efficacy and safety of fingolimod in patients with relapsing multiple sclerosis: a meta-analysis. *Br J Clin Pharmacol*. 2020:86:637–645. https://doi.org/10.1111/bcp.14198
11. Hyland MH, Cohen JA. Fingolimod. *Neurol Clin Pract*. 2011:1:61–65. https://doi.org/10.1212/CPJ.0b013e31823c51dd
12. Hagihara K et al. A genome-wide screen for FTY720-sensitive mutants reveals genes required for ROS homeostasis. *Microbial Cell (Graz, Austria)*. 2017:4:390–401. https://doi.org/10.15698/mic2017.12.601
13. Jalkh G, Abi Nahed R, Macaron G, Rensel M. Safety of newer disease modifying therapies in multiple sclerosis. *Vaccines (Basel)*. 2020:9:1–30. https://doi.org/10.3390/vaccines9010012
14. FDA. *Highlights of prescribing information*. Retrieved 2024 December 15, from https://www.accessdata.fda.gov/drugsatfda_docs/label/2024/022527s042lbl.pdf#page=26 (2010).
15. Mosmann T. Rapid colorimetric assay for cellular growth and survival: application to proliferation and cytotoxicity assays. *J Immunol Methods*. 1983:65:55–63. https://doi.org/10.1016/0022-1759(83)90303-4
16. Castiglione H et al. Development and optimization of a lactate dehydrogenase assay adapted to 3D cell cultures. *Organ*. 2024:3:113–125. https://doi.org/10.3390/organoids3020008
17. Repetto G, del Peso A, Zurita JL. Neutral red uptake assay for the estimation of cell viability/cytotoxicity. *Nat Protoc*. 2008:3:1125–1131. https://doi.org/10.1038/nprot.2008.75
18. Cossarizza A, Salvioli S. Flow cytometric analysis of mitochondrial membrane potential using JC-1. *Curr Protoc Cytom*. 2000:13:9–14. https://doi.org/10.1002/0471142956.cy0914s13
19. Szychowski KA, Rybczyńska-Tkaczyk K, Leja ML, Wójtowicz AK, Gmiński J. Tetrabromobisphenol a (TBBPA)-stimulated reactive oxygen species (ROS) production in cell-free model using the 2′,7′-dichlorodihydrofluorescein diacetate (H2DCFDA) assay-limitations of method. *Environ Sci Pollut Res*. 2016:23:12246–12252. https://doi.org/10.1007/s11356-016-6450-6
20. Beutler E, Duron O, Kelly BM. Improved method for the determination of blood glutathione. *J Lab Clin Med*. 1963:61:882–888
21. Çapan İ et al. Synthesis of novel carbazole hydrazinecarbothioamide scaffold as potent antioxidant, anticancer and antimicrobial agents. *BMC Chem*. 2024:18:102. https://doi.org/10.1186/s13065-024-01207-1
22. Hawash M, Jaradat N, Sabobeh R, Abualhasan M, Qaoud MT. New thiazole carboxamide derivatives as COX inhibitors: design, synthesis, anticancer screening, in silico molecular docking, and ADME profile studies. *ACS Omega*. 2023:8:29512–29526. https://doi.org/10.1021/acsomega.3c03256
23. Babalola BA, Adegboyega AE. Computational discovery of novel imidazole derivatives as inhibitors of SARS-CoV-2 main protease: an integrated approach combining molecular dynamics and binding affinity analysis. *COVID*. 2024:4:672–695. https://doi.org/10.3390/covid4060046
24. Friesner RA et al. Extra precision glide: docking and scoring incorporating a model of hydrophobic enclosure for protein-ligand complexes. *J Med Chem*. 2006:49:6177–6196. https://doi.org/10.1021/jm051256o
25. Adasme MF et al. PLIP 2021: expanding the scope of the protein-ligand interaction profiler to DNA and RNA. *Nucl Acid Res*. 2021:49:W530–W534. https://doi.org/10.1093/nar/gkab294
26. Kappos L et al. Oral fingolimod (FTY720) for relapsing multiple sclerosis. *N Engl J Med*. 2006:355:1124–1140. https://doi.org/10.1056/NEJMoa052643
27. Pournajaf S, Dargahi L, Javan M, Pourgholami MH. Molecular pharmacology and novel potential therapeutic applications of fingolimod. *Front Pharmacol*. 2022:13:807639. https://doi.org/10.3389/fphar.2022.807639
28. Norman BH. Drug induced liver injury (DILI). Mechanisms and medicinal chemistry avoidance/mitigation strategies. *J Med Chem*. 2020:63:11397–11419. https://doi.org/10.1021/acs.jmedchem.0c00524
29. Jaeschke H et al. Mechanisms of hepatotoxicity. *Toxicol Sci*. 2002:65:166–176. https://doi.org/10.1093/toxsci/65.2.166
30. Liao A et al. Autophagy induced by FTY720 promotes apoptosis in U266 cells. *Eur J Pharm Sci*. 2012:45:600–605. https://doi.org/10.1016/j.ejps.2011.12.014
31. Zhang L, Wang H, Ding K, Xu J. FTY720 induces autophagy-related apoptosis and necroptosis in human glioblastoma cells. *Toxicol Lett*. 2015:236:43–59. https://doi.org/10.1016/j.toxlet.2015.04.015
32. Hagihara K et al. Fingolimod (FTY720) stimulates Ca2+/calcineurin signaling in fission yeast. *PLoS One*. 2013:8:81907. https://doi.org/10.1371/journal.pone.0081907
33. Zhang N et al. FTY720 induces necrotic cell death and autophagy in ovarian cancer cells: a protective role of autophagy. *Autophagy*. 2010:6:1157–1167. https://doi.org/10.4161/auto.6.8.13614
34. Ahmed D, De Verdier PJ, Ryk C, Lunqe O, Flygare J. FTY720 (Fingolimod) sensitizes hepatocellular carcinoma cells to sorafenib-mediated cytotoxicity. *Pharma Res Per*. 2015:3:e00171. https://doi.org/10.1002/prp2.171
35. Hagihara K et al. FTY720 stimulated ROS generation and the Sty1/Atf1 signaling pathway in the fission yeast Schizosaccharomyces pombe. *Genes Cells*. 2014:19:325–337. https://doi.org/10.1111/gtc.12134
36. Redza-Dutordoir M, Averill-Bates DA. Activation of apoptosis signalling pathways by reactive oxygen species. *Biochim Biophys Acta*. 2016:1863:2977–2992. https://doi.org/10.1016/j.bbamcr.2016.09.012
37. Pessayre D, Mansouri A, Berson A, Fromenty B. Mitochondrial involvement in drug-induced liver injury. *Handb Exp Pharmacol*. 2010:196:311–365. https://doi.org/10.1007/978-3-642-00663-0_11
38. Gil A et al. Neuronal metabolism and neuroprotection: neuroprotective effect of fingolimod on menadione-induced mitochondrial damage. *Cells*. 2020:10:1–15. https://doi.org/10.3390/cells10010034
39. Martín-Montañez E et al. The S1P mimetic fingolimod phosphate regulates mitochondrial oxidative stress in neuronal cells. *Free Radic Biol Med*. 2019:137:116–130. https://doi.org/10.1016/j.freeradbiomed.2019.04.022
40. Raval K, Ganatra T. Basics, types and applications of molecular docking: a review. *IJCAAP*. 2022:7:12–16. https://doi.org/10.18231/j.ijcaap.2022.003

41. Han X et al. Bioinformatics analysis based on extracted ingredients combined with network pharmacology, molecular docking and molecular dynamics simulation to explore the mechanism of jinbei oral liquid in the therapy of idiopathic pulmonary fibrosis. *Heliyon*. 2024:10:e38173. https://doi.org/10.1016/j.heliyon.2024.e38173
42. Karaman B. *Application of computer-based methods to guide the development of novel sirtuin inhibitors*. (2015). https://opendata.uni-halle.de/bitstream/1981185920/8366/1/Berin_Karaman_PhD_Dissertation_CV_02_November_2015.pdf
43. Buler M, Aatsinki SM, Izzi V, Uusimaa J, Hakkola J. SIRT5 is under the control of PGC-1α and AMPK and is involved in regulation of mitochondrial energy metabolism. *FASEB J*. 2014:28:3225–3237. https://doi.org/10.1096/fj.13-245241
44. Guarente L. Sirtuins, aging, and metabolism. *Cold Spring Harb Symp Quant Biol*. 2011:76:81–90. https://doi.org/10.1101/sqb.2011.76.010629
45. Singh CK et al. The role of sirtuins in antioxidant and redox signaling. *Antioxid Redox Signal*. 2018:28:643–661. https://doi.org/10.1089/ars.2017.7290
46. Hirschey MD et al. SIRT3 regulates mitochondrial fatty-acid oxidation by reversible enzyme deacetylation. *Nature*. 2010:464:121–125. https://doi.org/10.1038/nature08778
47. Kong X et al. Sirtuin 3, a new target of PGC-1alpha, plays an important role in the suppression of ROS and mitochondrial biogenesis. *PLoS One*. 2010:5:e11707. https://doi.org/10.1371/journal.pone.0011707
48. Fiorentino F, Castiello C, Mai A, Rotili D. Therapeutic potential and activity modulation of the protein lysine deacylase sirtuin 5. *J Med Chem*. 2022:65:9580–9606. https://doi.org/10.1021/acs.jmedchem.2c00687
49. Nakagawa T, Lomb DJ, Haigis MC, Guarente L. SIRT5 deacetylates carbamoyl phosphate synthetase 1 and regulates the urea cycle. *Cell*. 2009:137:560–570. https://doi.org/10.1016/j.cell.2009.02.026
50. Park J et al. SIRT5-mediated lysine desuccinylation impacts diverse metabolic pathways. *Mol Cell*. 2013:50:919–930. https://doi.org/10.1016/j.molcel.2013.06.001
51. Fenton JJ. *Toxicology: a case-oriented approach*. (1st ed.). CRC Press, (2001), https://doi.org/10.1201/9781420042061
52. Ramachandran A, Visschers R, Duan L, Akakpo J, Jaeschke H. Mitochondrial dysfunction as a mechanism of drug-induced hepatotoxicity: current understanding and future perspectives. *J Clin Transl Res*. 2018:4:75–100. https://doi.org/10.18053/jctres.04.201801.005
53. Abdul NS, Nagiah S, Anand K, Chuturgoon AA. Molecular docking and mechanisms of fusaric acid induced mitochondrial sirtuin aberrations in glycolytically and oxidatively poised human hepatocellular carcinoma (HepG2) cells. *Toxicon*. 2020:173:48–56. https://doi.org/10.1016/j.toxicon.2019.11.009
54. Maya Ramírez CE et al. Identification of novel scaffolds targeting SIRT3 through molecular modeling techniques for the treatment of hepatocellular carcinoma. *J Biomol Struct Dyn*. 2024:42:10165–10174. https://doi.org/10.1080/07391102.2023.2256402
55. Wang HL et al. Interactions between sirtuins and fluorogenic small-molecule substrates offer insights into inhibitor design. *RSC Adv*. 2017:7:36214–36222. https://doi.org/10.1039/C7RA05824A
56. Yao J et al. Pyrazolone derivatives as potent and selective small-molecule SIRT5 inhibitors. *Eur J Med Chem*. 2023:247:115024. https://doi.org/10.1016/j.ejmech.2022.115024

Toxicology Research, 2025, **14**, 1–11
https://doi.org/10.1093/toxres/tfaf064
Paper